

Dual Photoactive Species in Glu46Asp and Glu46Ala Mutants of Photoactive Yellow Protein: A pH-Driven Color Transition[†]

Savitha Devanathan,[‡] Ronald Brudler,[§] Benedikt Hessling,^{||} Tammy T. Woo,[§] Klaus Gerwert,^{||} Elizabeth D. Getzoff,[§] Michael A. Cusanovich,[‡] and Gordon Tollin^{*;‡}

Department of Biochemistry, University of Arizona, Tucson, Arizona 85721, Department of Molecular Biology and Skaggs Institute for Chemical Biology, The Scripps Research Institute, La Jolla, California 92037, and Ruhr-Universität Bochum, Lehrstuhl für Biophysik, Universitätsstrasse 150, D-44780 Bochum, Germany

Received July 15, 1999

ABSTRACT: Photoactive yellow protein (PYP) is a blue light sensor present in the purple photosynthetic bacterium *Ectothiorhodospira halophila*, which undergoes a cyclic series of absorbance changes upon illumination at its λ_{\max} of 446 nm. The anionic *p*-hydroxycinnamoyl chromophore of PYP is covalently bound as a thiol ester to Cys69, buried in a hydrophobic pocket, and hydrogen-bonded via its phenolate oxygen to Glu46 and Tyr42. The chromophore becomes protonated in the photobleached state (I_2) after it undergoes trans-cis isomerization, which results in breaking of the H-bond between Glu46 and the chromophore and partial exposure of the phenolic ring to the solvent. In previous mutagenesis studies of a Glu46Gln mutant, we have shown that a key factor in controlling the color and photocycle kinetics of PYP is this H-bonding system. To further investigate this, we have now characterized Glu46Asp and Glu46Ala mutants. The ground-state absorption spectrum of the Glu46Asp mutant shows a pH-dependent equilibrium ($pK = 8.6$) between two species: a protonated (acidic) form ($\lambda_{\max} = 345$ nm), and a slightly blue-shifted deprotonated (basic) form ($\lambda_{\max} = 444$ nm). Both of these species are photoactive. A similar transition was also observed for the Glu46Ala mutant ($pK = 7.9$), resulting in two photoactive red-shifted forms: a basic species ($\lambda_{\max} = 465$ nm) and a protonated species ($\lambda_{\max} = 365$ nm). We attribute these spectral transitions to protonation/deprotonation of the phenolate oxygen of the chromophore. This is demonstrated by FT Raman spectra. Dark recovery kinetics (return to the unphotolyzed state) were found to vary appreciably between these various photoactive species. These spectral and kinetic properties indicate that the hydrogen bond between Glu46 and the chromophore hydroxyl group is a dominant factor in controlling the pK values of the chromophore and the glutamate carboxyl.

The photoactive yellow protein (PYP),¹ isolated from *Ectothiorhodospira halophila* (1), is a small, water-soluble, blue light transducing protein with a well-defined photocycle (2–4), for which a high-resolution crystal structure has been obtained (5). The key residues in the phototransducing machinery of PYP (Figure 1) are mainly localized within the binding site (5) for the thioester-linked *p*-hydroxycinnamoyl chromophore responsible for the blue light absorption in this protein ($\lambda_{\max} = 446$ nm). In the ground (dark-adapted) state, the trans form of the chromophore is stabilized as a result of its anionic oxygen being tethered to Glu46 and Tyr42 via hydrogen bonds. A series of structural changes

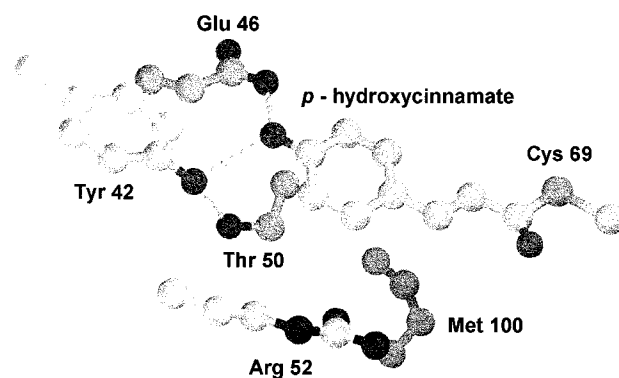


FIGURE 1: Key residues within the active site pocket of ground-state PYP.

[†] This work was supported by grants from the National Science Foundation (MCB-9722781) and from the National Institutes of Health (GM-37684).

* To whom correspondence should be addressed. E-mail: gtollin@u.arizona.edu. Fax: (520) 621-9288.

[‡] University of Arizona.

[§] The Scripps Research Institute.

^{||} Ruhr-Universität Bochum.

¹ Abbreviations: PYP, photoactive yellow protein; HEPES, *N*-(2-hydroxyethyl)-piperazine-*N'*-2-ethanesulfonic acid; MES, 2-(*N*-morpholino)ethanesulfonic acid; MOPS, 3-(*N*-morpholino)propanesulfonic acid; PCR, polymerase chain reaction; SDS-PAGE, sodium dodecyl sulfate-polyacrylamide gel electrophoresis.

following blue light absorption results in a characteristic trans-cis isomerization of the double bond in the chromophore, leading to breakage of the hydrogen bonds, protonation of the phenolate anion, and partial exposure of the phenolic ring to the solvent (6). Arg52, which shields the hydrophobic pocket containing the chromophore from solvent, moves out of the way and establishes a new hydrogen bond with the phenolic hydroxyl of the cis

chromophore (6). The photocycle is completed by a rate-limiting reversion of the chromophore, influenced by Met100 (7). Apparently, this sequence of steps relays the light signal to the transduction pathway involved in the presumed role of PYP in the negative phototactic response of *E. halophila* (8).

Site-specific mutagenesis has shown that Glu46 is one of the critical residues responsible for the photocycle kinetics and spectral tuning of the yellow color of PYP (9). The red-shifted 446 nm maximum of the ground-state absorption spectrum of PYP can be partially attributed to the anionic character of the chromophore phenolate oxygen, which is stabilized by the hydrogen bonding noted above, and which allows delocalization of the nonbonded electron pair into the pi-electron system. Further red-shifts in the absorption maximum have been observed with a Glu46Gln mutant (to 462 nm) (9), and a 3,4-dihydroxycinnamoyl (DH) variant chromophore (to 458 nm) (10). Even larger red-shifts were obtained for two PYP mutant-variants, Arg52Ala-DH (to 464 nm) and Glu46Gln-DH (to 470 nm) (11). Additionally, the Glu46Gln mutation resulted in very marked changes in the effects of pH on the photocycle kinetics (9).

The apparent increases in the anionic character of the chromophore phenolic oxygen (i.e., spectral red-shifts) thus far observed could be a direct consequence of changes in the hydrogen bonding interactions between the chromophore and its active site partners. To test this hypothesis and to extend our understanding of the role of Glu46 in PYP, we have constructed Glu46Asp and Glu46Ala mutants, so as to determine the effect of decreasing the length of the carbon chain and removing the carboxyl group in the side chain on the spectral and photocycle properties of PYP. As will be demonstrated below, the effects were quite dramatic and unexpected. Thus, the steady-state spectra of the dark-adapted states of the Glu46Asp and Glu46Ala mutants show the presence of a radically blue-shifted species (maxima at 345 and 365 nm, respectively) at neutral pH, in addition to a more normal wild-type-like PYP species, which is only slightly blue-shifted (to 444 nm) in the case of Glu46Asp, but is surprisingly red-shifted by ~20 nm (to 465 nm) for Glu46Ala. Furthermore, both the mutants participate in a pH-dependent transition between the two spectral forms. These differ in the protonation state of the chromophore hydroxyl group as demonstrated by Raman spectroscopy. Both of these forms of the mutants are photoactive, although they have quite different kinetic properties. The structural and mechanistic implications of these results are discussed.

MATERIALS AND METHODS

Site-Directed Mutagenesis. A PCR-based approach as implemented in the QuickChange kit (Stratagene) was used to generate the site-specific mutants. pPYP vector (9) was used as the template for PCR. The sequence of the primers for Glu46Asp was

```
5' AGTACAAGGCCGCGGACGGCGACATCACCG-
      GCCGCGACATCACCG 3'
5' TCATGTTCCGGCGCCTGCCGCTGTAGTGGCC-
      GGCGCTGTAGTGGC 3'
```

and for Glu46Ala was

```
5' AGTACAAGGCCGCGGCGGGCGACATCACCG-
      GCCGCGACATCACCG 3'
5' TCATGTTCCGGCGCCTGCCGCTGTAGTGGCC-
      GGCGCTGTAGTGGC 3'
```

The generation of the correct mutation was confirmed by DNA sequencing with an Applied Biosystems automated sequencer.

Protein Expression and Purification. Protein expression, chromophore attachment, and purification steps were as described previously (10). Purity and identity of the mutant proteins were verified by SDS-PAGE and mass spectrometry. The Glu46Asp mutant was approximately 95% pure, whereas the purity of the Glu46Ala mutant was >80%.

Steady-State and Time-Resolved Optical Spectroscopy. Steady-state UV-visible spectroscopy was performed on a Hewlett-Packard 8453 diode array spectrophotometer at room temperature. The dark recovery kinetic experiments for the Glu46Asp mutant were performed either on the diode array spectrophotometer or on an Olis-modified Cary 15 spectrophotometer. In the dark recovery experiments, the protein was first subjected to white light irradiation with a 100 W fiber optic illuminator for 3 min to ensure maximal conversion to the photobleached form; subsequently, the sample was placed in the dark, and absorption spectra were obtained every 30 s.

Laser flash photolysis and data analysis procedures for photocycle kinetic measurements were as described previously (2). The buffers used for various laser flash photolysis, steady-state photobleaching, and dark recovery experiments were either 10 mM Tris (pH 8.0), universal buffer (10 mM MES/MOPS/Bicine, pH 5.0–9.5), or 10 mM glycine (pH 8.5–10.5).

Fourier Transform (FT) Raman Spectroscopy. FT Raman spectroscopy was performed with an FRA 106 FT Raman module connected to an IFS 88 spectrometer (Bruker). The sample (4 mL of 40 mg/mL PYP in 20 mM HEPES at pH 7.0 or 20 mM glycine at pH 10.5) was pipetted into a specially designed quartz capillary (18) and put into the module. The sample was excited with a Nd:YAG laser (Adlas) at 1064 nm. A total of 8000–10 000 scans were averaged for each sample to improve the signal-to-noise ratio. The spectral resolution was $2 \pm 1 \text{ cm}^{-1}$. The measurements were performed at 22 °C. The spectra were corrected by subtraction of a buffer spectrum measured under identical conditions.

RESULTS

Effect of Mutations on Ground-State Absorption Spectra. The ground-state absorption spectrum of the Glu46Asp mutant shows a predominant 345 nm maximum below pH 7, and the appearance of a 444 nm maximum as the pH is raised above 7, with essentially complete conversion at pH 10.5 (Figure 2). At intermediate pH values, there is an equilibrium mixture of both chromophoric forms of the mutant. The clean isosbestic point at 390 nm indicates that only two light-absorbing species are present. The visible absorption spectrum of the basic form is slightly blue-shifted compared to wild-type PYP ($\lambda_{\text{max}} = 446 \text{ nm}$), whereas the spectrum of the protonated species is blue-shifted by 100 nm. (Figure 3 shows the resolved spectra compared to that

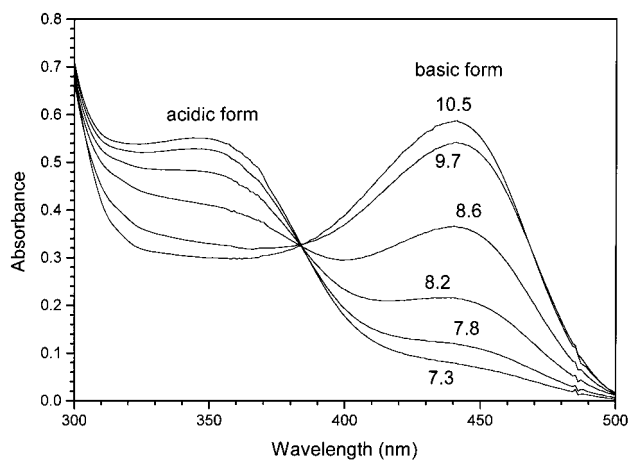


FIGURE 2: pH dependence of the absorption spectrum of the Glu46Asp mutant of PYP in 20 mM Tris buffer.

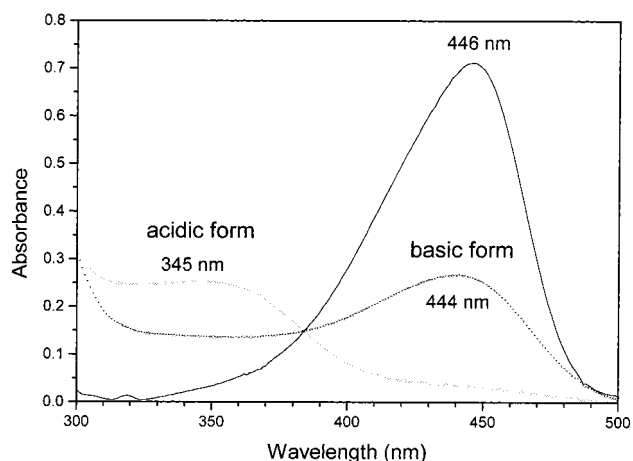


FIGURE 3: Absorption spectra of the acidic and basic forms of the Glu46Asp mutant of PYP obtained by subtracting the spectrum at pH 7.3 from that at pH 10.5. The spectrum of wild-type PYP is shown for comparison.

of wild-type PYP.) The pH dependence of the spectral changes is plotted in Figure 4. The transition is governed by a single proton equilibrium with a pK of 8.6.

The Glu46Ala mutant has a similar pH-dependent behavior involving two spectral forms. However, the wavelength maxima are shifted to 365 and 465 nm, respectively (i.e., 20 nm red-shifts in both bands relative to those in the Glu46Asp mutant), with a corresponding shift of the isosbestic point to 410 nm (data not shown). The pH dependence of the spectral changes in this mutant is governed by a single proton equilibrium with a pK of 7.9, as shown in Figure 4.

FT Raman Spectroscopy. The FT Raman spectrum of wild-type PYP exhibits bands at 1555, 1530, 1493, 1439, 1282, 1163, 1058, and 1043 cm^{-1} , in good agreement with a FT Raman spectrum of Kim et al. (1995). The FT Raman spectra of wild-type PYP and the mutant Glu46Asp at pH 10.5 are very similar with only minor band shifts of at most 5 cm^{-1} (Figure 5a,b). In contrast, the Raman spectrum of Glu46Asp at pH 7.0 is very different from the wild-type spectrum (Figure 5a,c). The main band at 1555 cm^{-1} (Figure 5a) is upshifted, and two peaks appear at 1597 and 1576 cm^{-1} . The band at 1493 cm^{-1} in wild-type PYP (Figure 5a) and at 1489 cm^{-1} in Glu46Asp at pH 10.5 (Figure 5b) is missing (Figure 5c), and the bands at 1439 and 1163/1161 cm^{-1} (Figure 5a,b) are shifted to 1446 and 1172 cm^{-1} , respectively.

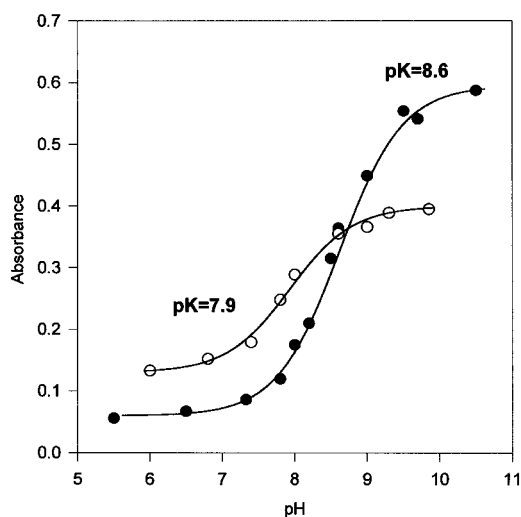


FIGURE 4: pH dependence of the amplitude of the absorbance at 444 nm for the basic form of the Glu46Asp mutant (closed circles) and at 465 nm for the basic form of the Glu46Ala mutant (open circles). Theoretical curves (solid lines) were obtained by fitting the data to the Hendersen-Hasselbach equation for the two data sets, corresponding to single proton ionizations with $pK = 8.6$ and 7.9, respectively.

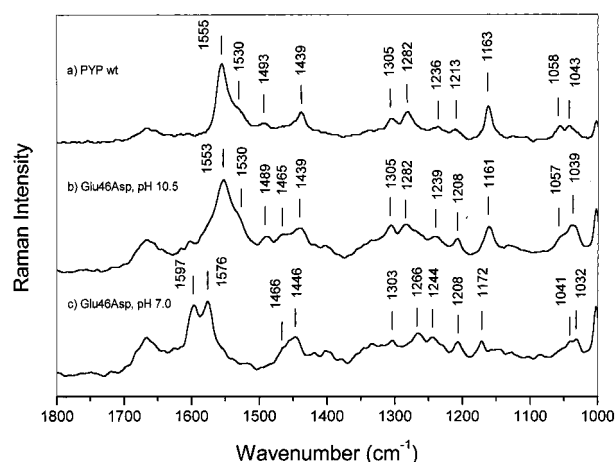


FIGURE 5: FT Raman spectra of (a) wild-type PYP at pH 10.5; (b) Glu46Asp mutant, pH 10.5; and (c) Glu46Asp mutant, at pH 7.0.

Also, the band at 1282 cm^{-1} (Figure 5a,b) appears shifted to 1266 cm^{-1} .

Steady-State Photobleaching and Recovery of the Glu46Asp Mutant. Steady-state illumination of the basic form of the Glu46Asp mutant at high pH results in bleaching of the 444 nm peak, which slowly recovers in the dark. The difference spectrum for the photobleaching at pH 9.5 is given in Figure 6, and clearly shows that the loss of the 444 nm species is accompanied by the formation of a 335 nm photobleached form (presumably corresponding to the 350 nm absorbing I_2 species obtained upon laser flash illumination of wild-type PYP; 2, 3). It is important to note that the spectrum of the 335 nm species is similar to that of the 345 nm acidic form of the mutant (see Figures 2 and 3), which is not present at this elevated pH. This suggests that the chromophore hydroxyl is protonated in both the 335 and 345 nm species, as it is in the I_2 intermediate (see below for further discussion). A series of spectra illustrating the time course of the dark recovery of the 444 nm absorption at pH 9.5 is shown in Figure 7. The first-order rate constant for this dark

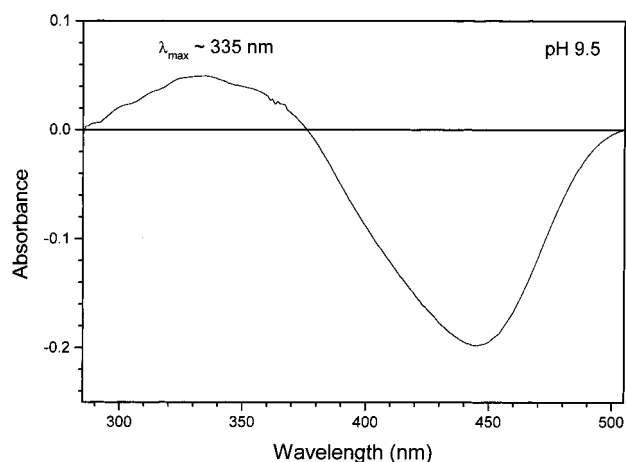


FIGURE 6: Steady-state difference spectrum for photobleaching of the basic form of the Glu46Asp mutant at pH 9.5 by irradiation with a 40 W fiber optic lamp.

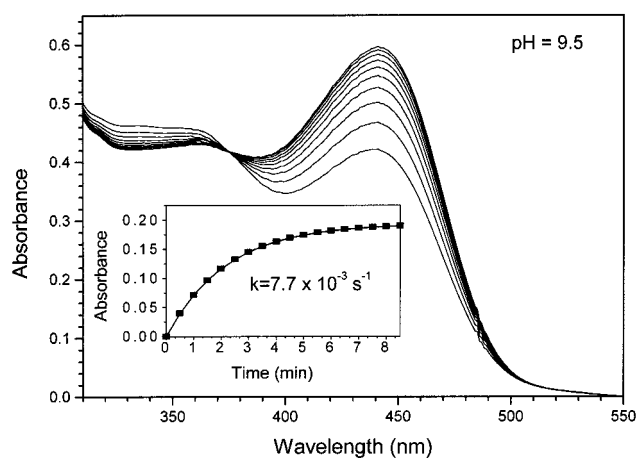


FIGURE 7: Dark recovery kinetics of the Glu46Asp mutant at pH 9.5 following steady-state bleaching by irradiation with a 40 W fiber optic lamp. Spectra taken at 30 s intervals. Note the isosbestic point at 385 nm. The inset shows the data points (closed squares) obtained at 444 nm superimposed on a single-exponential fit (solid line) with $k = 7.7 \times 10^{-3} \text{ s}^{-1}$.

Table 1: Rate Constants for Fast and Slow Conversions of I_2 to Ground State (pH 8.0) for Glu46-PYP Mutants

| mutant | $k_{\text{fast}} (\text{s}^{-1})$ | $k_{\text{slow}} (\text{s}^{-1})$ |
|-------------|-----------------------------------|-----------------------------------|
| Glu46Ala | | |
| basic form | 8.1×10^3 | 5.0×10^{-1} |
| acidic form | 7.5×10^3 | — |
| Glu46Asp | | |
| basic form | — | 2.6×10^{-3} |
| acidic form | 3.8×10^3 | — |

conversion of the I_2 intermediate back to the ground state (P) is $7.7 \times 10^{-3} \text{ s}^{-1}$ (inset). The Glu46Ala mutant does not show this steady-state photobleaching phenomenon because, as will be shown below, the dark recovery process is considerably faster and thus the I_2 species does not accumulate.

Time-Resolved Laser Flash Photolysis. The two spectral forms of the Glu46Asp mutant are both photoactive in laser flash photolysis experiments carried out at an intermediate pH of 8.0 (Table 1). The rate constants for laser-induced bleaching (i.e., conversion to the I_2 intermediate) for both species (data not shown) are too fast to measure with the present apparatus ($k > 10^6 \text{ s}^{-1}$; half-life $< 1 \text{ ms}$). The rate

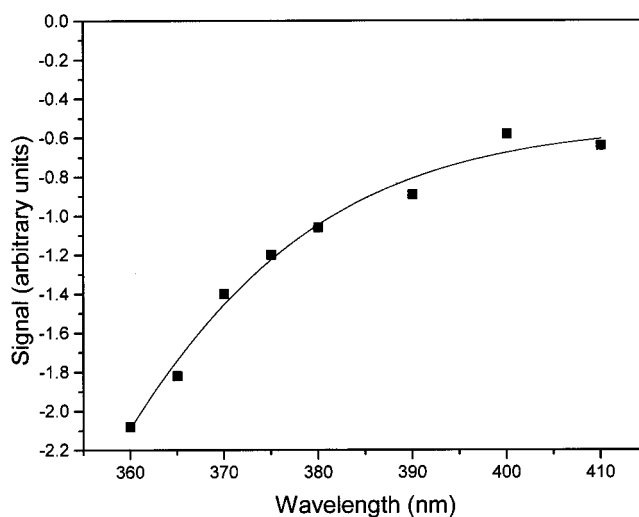


FIGURE 8: Flash-induced difference spectrum (excitation at $\lambda = 365 \text{ nm}$) for the acidic form of the Glu46Asp mutant at pH 6.5. Data were obtained at 5 ms after flash excitation.

constant for dark recovery (conversion of I_2 to P) of the 345 nm absorbing acidic species (data not shown) is $3.8 \times 10^3 \text{ s}^{-1}$ (half-life = $1.8 \times 10^{-4} \text{ s}$), which is 100 times faster than that for the wild-type protein, and 1.4×10^6 times faster than that for its 444 nm basic counterpart (for this species at pH 8.0, $k = 2.6 \times 10^{-3} \text{ s}^{-1}$, half-life = 266 s; this rate constant is about 2000-fold smaller than that for wild-type PYP). A time-resolved difference spectrum for laser flash-induced photobleaching of the acidic form is shown in Figure 8. The difference spectrum clearly reveals absorbance bleaching in the 360 nm wavelength region, although absorbance changes at wavelengths below 360 nm were not measurable with the present apparatus.

Photobleaching kinetics for the Glu46Ala mutant were also too fast to measure. However, the dark recovery kinetics after laser photobleaching of the 465 nm basic form of this mutant (at pH 8.0) showed a biphasic process, with a partial fast recovery ($k = 8.1 \times 10^3 \text{ s}^{-1}$; half-life = $8.6 \times 10^{-5} \text{ s}$) and a slower complete recovery ($k = 0.5 \text{ s}^{-1}$; half-life = 1.4 s) (data not shown). The fast recovery component for the basic form of this Glu46Ala mutant occurs approximately 10^6 times faster than that of the Glu46Asp mutant (but is comparable to its 365 nm acidic form, for which at pH 8.0, $k = 7.5 \times 10^3 \text{ s}^{-1}$; half-life = $9.2 \times 10^{-5} \text{ s}$), whereas the slower recovery phase occurs on the same time scale as wild-type PYP and is 200 times faster than that of the Glu46Asp mutant. The rate constants for these dark recovery processes have been compiled in Table 1.

pH-Dependent Recovery Kinetics of the Photobleached Acidic Forms. The pH dependence of the flash-induced kinetics for dark recovery of the 345 nm acidic form (Figure 9) of the Glu46Asp mutant shows a maximum recovery rate at pH 6.5 ($k = 12.5 \times 10^3 \text{ s}^{-1}$, half-life = $5.5 \times 10^{-5} \text{ s}$), which decreased 10-fold as the pH was increased to 9.5, and decreased 3-fold as the pH was decreased to 5.5 (below pH 5.5, a decrease in protein stability was noted). This biphasic curve is governed by pK values of ≈ 6 and ≈ 7.5 , and resembles the biphasic pH dependence of the dark recovery kinetics of I_2 in wild-type PYP, which has pK values of 6.4 and 9.4 (9). The Glu46Ala mutant shows similar biphasic behavior exhibiting pK values of ≈ 7.3 and ≈ 8.6 (Figure 9).

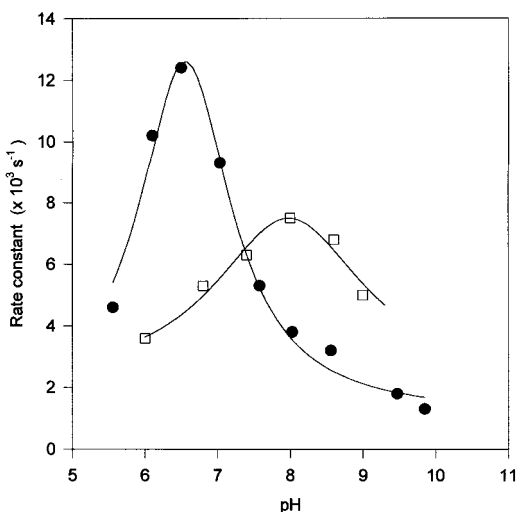


FIGURE 9: Effect of pH on the flash-induced dark recovery kinetics of the 345 nm acidic form of the Glu46Asp mutant (closed circles) and of the 365 nm acidic form of the Glu46Ala mutant (open squares).

The maximum rate of recovery for the Glu46Ala mutant occurs at pH 8 ($k = 7.5 \times 10^3 \text{ s}^{-1}$; half-life = $0.92 \times 10^{-4} \text{ s}$), a shift of ~ 2 pK units from the Glu46Asp mutant. The groups responsible for these pH effects are not yet identified.

pH-Dependent Recovery Kinetics of the Photobleached Basic Forms. The rate constant for the dark recovery of the photobleached 444 nm basic form of the Glu46Asp mutant increased 6-fold with pH, from $k = 2.6 \times 10^{-3} \text{ s}^{-1}$ (half-life = 266 s) at pH 8.0 to $k = 0.017 \text{ s}^{-1}$ (half-life = 42 s) at pH 10.5 (Figure 10a). The pH dependence follows a single proton ionization curve with a $pK = 9.6$. Even at these elevated pHs, the mutant was found to be remarkably stable, based on absorption spectral measurements. These dark recovery kinetics were several hundred times slower than for wild-type PYP and resemble those of the Met100Ala mutant (7).

The kinetics of the faster dark recovery phase of the Glu46Ala mutant have a pK of ≈ 9.5 (Figure 10b), whereas the slower recovery process showed a pK of 9.0 (Figure 10b). Note that these pK values are similar to that observed for Glu46Asp. The rate constants for the slower full recovery ranged from $k = 0.45 \text{ s}^{-1}$ (half-life = 1.5 s) at pH 8 to $k = 1.55 \text{ s}^{-1}$ (half-life = 0.45 s) at pH 10, an increase of ~ 4 -fold between the two extreme pHs.

Lack of Photorecovery of the Photobleached 444 nm Basic Form of the Glu46Asp Mutant. To test whether the long-lived photobleached state (I_2 intermediate) of the 444 nm basic form of the Glu46Asp mutant could be photoconverted to the ground state, as was previously observed for the Met100Ala mutant (7), the 444 nm form at pH 9.0 was first photobleached by irradiation with a 40 W tungsten lamp for 3 min, and then was excited at 360 nm with a laser pulse. There was no rapid recovery of absorbance at 444 nm. This experiment could not be carried out for the Glu46Ala mutant because the recovery process was too rapid to permit the build-up of the photobleached species.

DISCUSSION

As demonstrated above, mutation of PYP Glu46 to either Asp or Ala results in pH-titratable species in which the

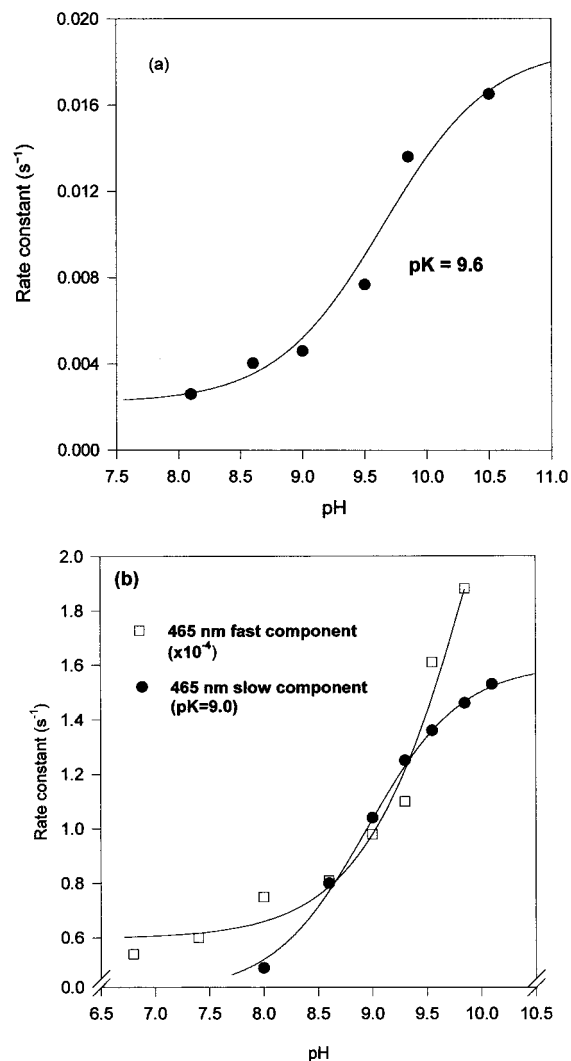


FIGURE 10: (a) pH dependence of the dark recovery kinetics (closed circles) of the photobleached (I_2) basic form of the Glu46Asp mutant. A theoretical curve (solid line) was obtained by fitting the data to the Henderson–Hasselbach equation for a single proton ionization with a pK of 9.6. (b) Effect of pH on the fast component (open squares) and slow component (closed circles) of the flash-induced dark recovery kinetics for the basic form of the Glu46Ala mutant, measured at 465 nm. A theoretical curve (solid line) was obtained by fitting the data for the slow component to the Henderson–Hasselbach equation for a single proton ionization with a pK of 9.0. The curve drawn through the open squares is an arbitrary fit to the data points.

chromophore in the dark-adapted state can be converted from a basic form (absorbing at 444 or 465 nm) to an acidic form (absorbing at 345 or 365 nm), with pK values of 8.6 (Glu46Asp) and 7.9 (Glu46Ala). We attribute this to a conversion of the chromophore hydroxyl group from an anionic to a protonated form. The FT Raman spectra are consistent with this interpretation. Using the chromophore model compound *p*-hydroxycinnamoyl phenyl thioester, Kim et al. (1995) have shown that the bands at 1555, 1530, 1493, 1439, and 1163 cm^{-1} in wild-type PYP (Figure 5a) are indicative for the deprotonated chromophore. These bands are present in the mutant Glu46Asp at pH 10.5 at 1553, 1530, 1489, 1439, and 1161 cm^{-1} (Figure 5b) and indicate that the chromophore in Glu46Asp at high pH is also deprotonated. The resonance Raman spectrum of the chromophore model compound in its anionic form shows corresponding

bands at 1568, 1542, 1500, 1434, and 1166 cm^{-1} (12). In the neutral model compound, however, the most intense bands at 1568 and 1542 cm^{-1} upshift to 1600 and 1587 cm^{-1} , the band at 1500 cm^{-1} is missing, the intensity of the band at 1434 cm^{-1} appears strongly reduced, and the band at 1166 cm^{-1} is shifted to 1176 cm^{-1} (12). The upshift of the most intense bands to 1597/1576 cm^{-1} , the absence of the band at 1493 cm^{-1} , and the band shift from 1163 to 1172 cm^{-1} for the Glu46Asp mutant at neutral pH (compare Figures 5a and 5c) are similar to the neutral model compound. We conclude from these results that the chromophore in Glu46Asp at pH 7.0 is protonated and possibly exposed to the aqueous environment. We presume that the same interpretation is valid for the Glu46Ala mutant, although we have not carried out the corresponding FT Raman experiments.

This behavior is in sharp contrast to wild-type PYP, for which the chromophore becomes protonated only upon protein denaturation, with an apparent pK of 2.7 (1, 13). This difference of ~ 6 pH units for the protonation of the chromophore indicates that hydrogen bonding from the Glu46 carboxyl group stabilizes the anionic form of the chromophore to a much greater extent than such an interaction with the carboxyl of the Asp46 mutant. The hydrophobic replacement in the Glu46Ala mutant, of course, completely eliminates the possibility of H-bond formation. In the Glu46Asp mutant, the hydrogen bonding distance between the phenolic oxygen of the chromophore and the Asp carboxyl group is probably increased due to the decrease in the length of the side chain by one carbon, as well as by possible steric interference between the Asp carboxyl and the phenol ring of Tyr42, thereby weakening or eliminating this hydrogen bond. The small difference between the pK values of the Asp and Ala mutants for chromophore protonation suggests that neither Asp46 nor Ala46 appreciably stabilizes the anionic chromophore. Presumably, in both mutants the H-bond to Tyr42 remains intact and can therefore provide some degree of stabilization.

It is not clear why the anionic form of the chromophore in the Glu46Ala mutant has a spectrum which is shifted 20 nm to the red compared to wild-type PYP, whereas the Glu46Asp mutant is slightly blue-shifted to 444 nm. Perhaps changes in the environment around the chromophore, such as the extra space that is created on truncating the Glu46 side chain, result in polarity changes which contribute to these spectral shifts. An improved understanding of these properties may be obtained from crystallographic analysis of these mutants. Such studies are underway.

It is interesting that the acidic forms remain photoexcitable; i.e., they can be additionally bleached by light, presumably to generate its isomeric conformer. Whether this is a trans to cis conversion, or the opposite, is not clear at present.

It is noteworthy that the pK observed for the rate constant of the recovery of the photobleached form of the anionic species of both mutants is approximately the same as that found for protonation of the free chromophore ($pK = 9.0$; 14). This indicates that the chromophore phenolic oxygen is readily accessible to the solvent in the photobleached state, and that removal of the proton from the phenolic oxygen facilitates recovery. The 200 times faster recovery rate for Glu46Ala than for Glu46Asp suggests that the Asp46 carboxyl is probably negatively charged at the higher pH values, thus hindering the return of the anionic chromophore

into the active site. Conversely, protonation of the Asp46 carboxylate at the lower pH values could account for the more rapid recovery rates observed with this species.

It has been suggested that during the formation of the I_2 intermediate in the PYP photocycle Glu46 donates a proton to the phenolic oxygen of the chromophore (15, 16). This is based upon low-temperature steady-state infrared difference spectroscopy. The Glu46Gln mutant, however, is able to undergo a highly efficient photocycle, at neutral pH, with kinetics qualitatively similar to those of the wild-type protein (9). We conclude from these results that, at the very least, proton donation from Glu46 to the chromophore is not a required component of the PYP photocycle.

The recovery kinetics for the 444 nm form of the Glu46Asp mutant were dramatically slowed compared to wild-type PYP, and resemble those of the Met100Ala mutant (for which $k = 2.1 \times 10^{-3} \text{ s}^{-1}$; half-life = 330 s at pH 7.0; 7). We previously proposed that Met100 aids the reisomerization of the chromophore and that its absence is responsible for the slow recovery of the Met100Ala mutant. This, of course, cannot be true for the Glu46Asp mutant. A possible explanation is that the carboxyl group of the Asp46 residue has a negative charge in the photobleached state and has to be protonated by the solvent before the anionic chromophore reisomerizes; i.e., the active site may not allow two negative charges to be present, thereby slowing down the recovery process. This could explain why the rate of recovery for the Glu46Ala mutation is almost comparable to wild-type PYP, since this mutant does not have any charged residue in the hydrophobic pocket to prevent the anionic chromophore from reestablishing the H-bond with Tyr42.

Further insight regarding the mechanistic aspects of the back-reaction (I_2 to P) is obtained from the fact that the photobleached Glu46Asp mutant did not show enhanced rates of photorecovery when a second laser pulse at 360 nm was used. This is consistent with the observation that the Met100 residue is present in this mutant. Since this residue may be involved in facilitating the reisomerization process (7), the chromophore would already be in the trans conformation, and light absorption and therefore double bond isomerization would not be required for recovery of the dark-adapted state. Based on these considerations, it is interesting to speculate on the mechanism by which Met100 might be involved in the reisomerization reaction. The structure of the photobleached state obtained by X-ray diffraction (6) shows that the occupied p-orbital of the Met S atom is oriented toward C_7 of the cis conformation of the chromophore (the distance between the two atoms is 4.9 Å), and the Met sulfur atom is also within van der Waals distance of the slightly twisted benzene ring of the chromophore. The electron density on the Met sulfur atom could be further increased by interacting with the pi-orbital of the benzene ring. This in turn can result in charge donation to C_7 of the cis double bond, thereby causing a decrease in its double bond character and facilitating rotation about this bond, which is required for I_2 to reisomerize and return to the ground state.

CONCLUSIONS

Glu46Asp and Glu46Ala are the first PYP mutants to be characterized that show dual photoactive species, a result of a pH-driven color transition. At pH < 8.0 , photoactive 345/

365 nm species are predominant, with properties suggesting that all active site residues are protonated, and that the chromophore is present in its trans conformation. Above pH 9.0, a 444 nm form is present in the Glu46Asp mutant, which is spectrally similar to the wild-type protein, but whose anionic form of the chromophore is considerably less stabilized by Asp than it is by Glu. The slowing of the recovery rate by a factor of 2000 and the change in pK for chromophore protonation from ≤ 2.7 in the wild-type to 8.6 in the mutant are indicative of this destabilization. It is interesting that eliminating the H-bond by replacement of Asp by Ala apparently increases the anionic character of the chromophore, resulting in a 20 nm red-shifted absorption spectrum, although the pK of 7.9 for protonation still shows destabilization relative to the wild-type protein.

The dramatic 10^6 -fold difference in recovery kinetics between the two chromophoric forms of the Glu46Asp mutant can be explained on the basis that the phenolic oxygen atom of the protonated chromophore in the acidic form does not have to lose its proton before it returns into the active site, as is the case for the 444 nm form. Presumably, this is a kinetically difficult process in the latter species, since the carboxyl of the Asp mutant is probably deprotonated at the high pH values required to form the 444 nm basic form and thus hinders the return of the chromophore. The recovery of the 465 nm basic form of the Glu46Ala mutant can proceed faster because of the lack of an additional negative charge. These structural predictions for the two photoactive forms of the Glu46 mutants can be tested by crystal structure determinations for both of these species. Such studies are underway.

ACKNOWLEDGMENT

We thank Dr. Terry Meyer for a critical review of the manuscript and Nicoleta Constantin and Dr. Mark Dodson for technical assistance with gel electrophoresis.

REFERENCES

- Meyer, T. E. (1985) *Biochim. Biophys. Acta* 806, 175–183.
- Meyer, T. E., Yakali, E., Cusanovich, M. A., and Tollin, G. (1987) *Biochemistry* 26, 418–423.
- Meyer, T. E., Tollin, G., Hazzard, J. H., and Cusanovich, M. A. (1989) *Biophys. J.* 56, 559–564.
- Ujj, L., Devanathan, S., Meyer, T. E., Cusanovich, M. A., Tollin, G., and Atkinson, G. H. (1998) *Biophys. J.* 75, 406–412.
- Borgstahl, G. E. O., Williams, D. R., and Getzoff, E. D. (1995) *Biochemistry* 34, 6278–6287.
- Genick, U. K., Borgstahl, G. E. O., Ng, K., Ren, Z., Pradervand, C., Burke, P. M., Srajer, V., Teng, T., Schildkamp, W., McRee, D. E., Moffat, K., and Getzoff, E. D. (1997) *Science* 275, 1471–1475.
- Devanathan, S., Genick, U. K., Canestrelli, I. L., Meyer, T. E., Cusanovich, M. A., Getzoff, E. D., and Tollin, G. (1998) *Biochemistry* 37, 11563–11568.
- Sprenger, W. W., Hoff, W. D., Armitage, J. P., and Hellingwerf, K. J. (1993) *J. Bacteriol.* 175, 3096–3104.
- Genick, U. K., Devanathan, S., Meyer, T. E., Canestrelli, I. L., Williams, E., Cusanovich, M. A., Tollin, G., and Getzoff, E. D. (1997) *Biochemistry* 36, 8–14.
- Devanathan, S., Genick, U. K., Getzoff, E. D., Meyer, T. E., Cusanovich, M. A., and Tollin, G. (1997) *Arch. Biochem. Biophys.* 340, 83–89.
- Devanathan, S., Genick, U. K., Canestrelli, I. L., Getzoff, E. D., Meyer, T. E., Cusanovich, M. A., and Tollin, G. (1997) in Forty-first Annual Meeting of the Biophysical Society.
- Kim, M., Mathies, R. A., Hoff, W. D., and Hellingwerf, K. J. (1995) *Biochemistry* 34, 12669–12672.
- Hoff, W. D., Van Stokkum, I. H. M., Gural, J., and Hellingwerf, K. J. (1997) *Biochim. Biophys. Acta* 1322, 151–162.
- Baca, M., Borgstahl, G. E. O., Boissinot, M., Burke, P. M., Williams, D. R., Slater, K. A., and Getzoff, E. D. (1994) *Biochemistry* 33, 14369–14377.
- Xie, A., Hoff, W. D., Kroon, A. R., and Hellingwerf, K. J. (1996) *Biochemistry* 35, 14671–14678.
- Imamoto, Y., Mihara, K., Hisatomi, O., Kataoka, M., Tokunaga, F., Bojkova, N., and Yoshihara, K. (1997) *J. Biol. Chem.* 272, 12905–12908.
- Meyer, T. E., Cusanovich, M. A., and Tollin, G. (1993) *Arch. Biochem. Biophys.* 306, 515–517.
- Hessling, B. (1996) Ph.D. Thesis, Ruhr University, Bochum. BI991634P